



HAL
open science

Study of the relationship between red wine colloidal fraction and astringency by asymmetrical flow field-flow fractionation coupled with multi-detection

Kevin Pascotto, Coline Leriche, Soline Caillé, Frédéric Violleau, Jean-Claude Boulet, Olivier Geffroy, Cécile Levasseur-Garcia, Veronique Cheynier

► **To cite this version:**

Kevin Pascotto, Coline Leriche, Soline Caillé, Frédéric Violleau, Jean-Claude Boulet, et al.. Study of the relationship between red wine colloidal fraction and astringency by asymmetrical flow field-flow fractionation coupled with multi-detection. *Food Chemistry*, 2021, 361, pp.130104. <10.1016/j.foodchem.2021.130104>. <hal-03300210>

HAL Id: hal-03300210

<https://hal.inrae.fr/hal-03300210v1>

Submitted on 6 Jun 2023

HAL is a multi-disciplinary open access archive for the deposit and dissemination of scientific research documents, whether they are published or not. The documents may come from teaching and research institutions in France or abroad, or from public or private research centers.

L'archive ouverte pluridisciplinaire HAL, est destinée au dépôt et à la diffusion de documents scientifiques de niveau recherche, publiés ou non, émanant des établissements d'enseignement et de recherche français ou étrangers, des laboratoires publics ou privés.



Distributed under a Creative Commons CC BY-NC-ND 4.0 - Attribution - Non-commercial use - No Derivative Works - International License

1 **Study of the relationship between red wine colloidal fraction and**
2 **astringency by Asymmetrical Flow Field-Flow Fractionation**
3 **coupled with multi-detection**

4

5 Kevin Pascotto^{a,b}, Coline Leriche^e, Soline Caillé^c, Frédéric Violleau^{a,b}, Jean-Claude Boulet^{c,d}, Olivier
6 Geffroy^a, Cécile Levasseur^a and Véronique Cheynier^c

7

8 ^a Plateforme TFFFC, Université de Toulouse, INP-PURPAN, Toulouse, France

9 ^b Laboratoire de Chimie Agro-industrielle, LCA, Université de Toulouse, INRAE, Toulouse, France

10 ^c SPO, INRAE, Univ Montpellier, Institut Agro, Montpellier, France

11 ^d INRAE, PROBE Research Infrastructure, Polyphenol Analytical Facility, Montpellier, France

12 ^e INRAE, UE999 Pech-Rouge, Gruissan, France

13

14 **Abstract**

15 Macromolecules including condensed tannins and polysaccharides impact wine taste and especially
16 astringency. Asymmetrical Flow-Field-Flow-Fractionation (AF4) coupled to UV detection (UV),
17 multi-angle light scattering (MALS) and refractive index detection (dRI) has been proposed to
18 separate red wine colloids.

19 The present work aimed at relating AF4-multidetector profiles with red wine astringency. Fifty
20 commercial red wines characterized by a trained sensory panel were analysed by AF4-UV-MALS-dRI
21 and UV-visible spectroscopy. The analytical data set was built by selecting the three variables most
22 predictive of the astringency score from each table (UV, dRI, MALS, M_w distribution, and UV-visible
23 spectra of whole wine, permeate and retentate AF4 fractions) and analysed by principal component
24 analysis. Red wine astringency was more related to variables extracted from the AF4 data than to UV-
25 absorbance of the wine or permeate, confirming the relevance of AF4-multidetector for analysis of
26 the colloidal fraction involved in this perception.

27

28 **Key words:** wine, astringency, polyphenols, macromolecules, AF4-UV-MALS-dRI, chemometrics

29

30

1. Introduction

31 Astringency is one of the major sensory attributes of red wines. It is defined as dryness, tightening,
32 and puckering sensations perceived in the oral cavity during the intake of astringent compounds
33 (Soares et al., 2020). Polyphenolic compounds and especially tannins are known to be involved in red
34 wine astringency (Gawel, 1998). This perception is generally attributed to the capacity of tannins to
35 bind salivary proteins, leading to the formation of precipitates which reduce the lubrication in the
36 mouth (Bate-Smith, 1973; Baxter, Lilley, Haslam, & Williamson, 1997; McRae & Kennedy, 2011).

37 Perceived astringency increases with tannin molecular weight (degree of polymerization) (Peleg,
38 Gacon, Schlich, & Noble, 1999; Vidal et al., 2003), their number of galloyl substituents (galloylation
39 degree) (Vidal et al., 2003) and their concentration (Vidal, Courcoux, et al., 2004). Red wine
40 astringency was reported to be primarily associated with a fraction containing higher molecular weight
41 phenolics (> 5 kDa) (Hufnagel & Hofmann, 2008a, b) although some lower molecular weight
42 phenolics (e.g. phenolic acids and their ethyl esters, flavan-3-ol monomers and oligomers, flavonol
43 and dihydroflavonol glycosides) also exhibited astringency (Ferrer-Gallego, Hernández-Hierro, Rivas-
44 Gonzalo, & Escribano-Bailón, 2014; Hufnagel & Hofmann, 2008b; Peleg et al., 1999; Vidal et al.,
45 2018).

46 Polysaccharides constitute another important group of wine macromolecules (Pellerin, Vidal, Williams
47 & Brillouet, 1995). They comprise polysaccharides rich in arabinose and galactose (PRAGs), and
48 rhamnogalacturonan II (RGII) originating from grape cell walls (Pellerin, Vidal, Williams, &
49 Brillouet, 1995), and mannoproteins (MPs) from yeast cell walls. These compounds are known to
50 interact with tannin perception, reducing astringency both in model solutions (Le Bourvellec &
51 Renard, 2012; Vidal et al., 2004), and in red wines (Boulet et al., 2016; Quijada-Morín, Williams,
52 Rivas-Gonzalo, Doco, & Escribano-Bailón, 2014).

53 Astringency perception results from a complex system involving multiple factors. Some works based
54 on chemometrics approach modelled analytical data to explain the sensory impact of chemical
55 compounds, considering many factors. Several authors used multivariate analysis (Quijada-Morín et

56 al., 2014) such as multiple linear regression (MLR) (Boulet et al., 2016; Quijada-Morín et al., 2014),
57 or partial least squares regression (PLSR) (Preys et al., 2006), to cross instrumental and sensory data
58 for describing the relationships between several groups of variables. For example, the smoothing
59 capacity of wine polysaccharides was confirmed using chemometrics tools (principal component
60 analysis, PCA and multiple linear regression, MLR) (Boulet et al., 2016; Quijada-Morín et al., 2014).
61 Additionally, it was shown that the absorbance values at $\lambda = 230$ nm efficiently predict the perceived
62 astringency in wine (Boulet et al., 2016). However, these studies did not consider the apparent molar
63 mass of compounds. Other works assessed the impact of individual phenolic compounds quantified by
64 HPLC-DAD (Kallithraka, Kim, Tsakiris, Paraskevopoulos, & Soleas, 2011) and HPLC-DAD-MS
65 (Vidal et al., 2018). Nevertheless, neither higher molecular weight polyphenols nor polysaccharides
66 were considered in their models. Tannin composition is classically determined by HPLC after
67 depolymerisation in the presence of a nucleophilic reagent (e.g. thiolysis, phloroglucinolysis).
68 However, when applied to wine, these methods do not predict astringency unlike more global methods
69 such as BSA precipitation (Boulet et al., 2016; Harbertson & Kennedy, 2002), or spectrophotometric
70 measurements (Boulet et al., 2016).

71 A method based on Asymmetrical – Flow – Field – Flow – Fractionation (AF4), coupled to a multi-
72 detection system consisting of UV detection (UV), multi-angle light scattering (MALS), and
73 differential refractometer index (dRI) (AF4-UV-MALS-dRI), using a wine like solution as the mobile
74 phase has been recently developed (Pascotto, Cheynier, Williams, Geffroy, & Violleau, 2020). This
75 method allowed separation of wine macromolecules into four fractions. The first three were assigned
76 to higher M_w tannins coeluted with lower M_w polysaccharides such as rhamnogalacturonan II (F1), to
77 intermediate M_w polysaccharides such as polysaccharides rich in arabinan and galactan (PRAGs) (F2),
78 and to higher M_w mannoproteins (F3) whereas the last fraction (F4) was not identified (Pascotto et al.,
79 2020). Moreover, Marassi and coworkers reported the presence of residual proteins in the low
80 retention time fractions (Marassi et al., 2021).

81 The hypothesis of the present study was that the AF4 multi-detection profiles obtained with the
82 method developed in our earlier paper (Pascotto et al., 2020) are related to red wine astringency. To

83 evaluate whether the method is relevant to analyse the wine colloids contributing astringency (i.e.
84 tannins) or mitigating it (e.g. polysaccharides), AF4 analysis was performed on a series of red wines
85 from Languedoc region (France) which were tasted by a sensory panel using QDA procedure. The two
86 data sets (analytical and sensory) were then processed using multiway analysis to assess the potential
87 of A4F profiles for prediction of wine astringency and determine the contribution of the different A4F
88 fractions.

89 **2. *Materials and methods***

90 **2.1. Wine collection**

91 In this work, fifty red wines produced in 2016 in several Protected Denominations of Origin (PDOs)
92 from the French Languedoc area (Corbières-Boutenac, la Clape, Faugères, Minervois-Terrasses de
93 l'Argent Double, Languedoc-Montpeyroux and Pic-Saint-Loup) were used. Most of the samples were
94 blended wines mainly made from Grenache, Syrah and Carignan and are sold between 5 and 20 euros.
95 Wines from the PDO Corbières-Boutenac were barrel aged. Wines were coded 1 to 50 as summarized
96 in Table S1. Fifteen bottles of each wines were used for the sensory analysis, one bottle for the
97 chemical analysis.

98 **2.2. Sensory analysis**

99 The wines were evaluated using Quantitative Descriptive Analysis (Stone & Sidel, 2004) QDA® in
100 2019 by a trained panel from the Sensory Laboratory of UMR SPO, INRAE (Montpellier, France).
101 This panel was composed of 18 judges unrelated to the wine industry (genders: 12 women, 6 men;
102 average age: 55 years old; seniority on the panel: 5 years in average - 3 months minimum - 13 years
103 maximum). The selection of these judges was based on their sensory performances and their ability to
104 communicate in group (Depledt, 2009; Nicod, 1998). After three sessions for vocabulary generation
105 on the 50 wines, the panel considered 16 independent and discriminating descriptors, including
106 astringency (Depledt, 2009). Judges were trained during a one-hour session on the perception of
107 astringency. A grape seed and stalk tannin extract was added to wine sample as a training standard for
108 astringency assessment. A range of concentrations was presented to the panel: 0 – 0.6 and 0.8 g.L⁻¹,

109 and the judges were asked to classify these samples according to the astringency intensity. As a final
110 training step, a Feedback Calibration Method was used in order to check if the panel performances
111 were strong enough to characterize the wines efficiently (Findlay, Castura, Schlich, & Lesschaeve,
112 2006). For the rating, wines were presented in a monadic service according to a Latin square of
113 Williams (Macfie, Bratchell, Greenhoff, & Vallis, 1989), served in black glasses, at room temperature
114 with a plastic cup over glasses to keep aromas. Judges evaluated the wines in standard tasting cabs and
115 rated the intensity of each descriptor on linear scales, from low corresponding to absence of perception
116 to high corresponding to very intense perception, for each wine. The distances on the linear scale are
117 then converted to scores (from 0 to 10) for statistical analyses. Judges were invited to rinse their mouth
118 with a solution of pectin (1 g.L^{-1}) then with water between each sample in order to limit the carry over
119 effect of astringency of red wines (Colonna, Adams & Noble, 2004). Six sessions were dedicated to
120 the rating: one session for each PDO. At the end, the repeatability of the panel was tested
121 independently, considering two wines from each PDO, with a repetition in the same session.
122 Astringency intensities were then extracted from the QDA data.

123 **2.3. AF4 analysis**

124 *2.3.1. Chemical*

125 Ultrapure water was obtained from a Merck MilliQ integral 15 system. Ethanol, methanol, formic acid
126 and HCl (99% purity, HPLC grade) were purchased from Carlo Erba (France). Sodium azide and
127 sodium nitrate (99.5% purity) were purchased from Sigma Aldrich (St Louis, MO, USA). Potassium
128 sulphate was obtained from Merck (Darmstadt, Germany) and has a purity at 99%. Bovine serum
129 albumin (BSA) was purchased from Thermo Scientific (USA) and prepared at 2 mg/ml in a 0.9%
130 NaCl solution (m/v).

131 *2.3.2. Sample preparation*

132 Wine aliquots (1 mL) were dried with a Genevac EZ-2plus evaporator under reduced pressure at 8
133 mbars at 40°C and stored at -80 °C until used to limit evolution. Then, dried wine was dissolved in 1
134 mL of a wine like solution (water/ethanol – 88/12, v/v) with a pH adjusted to 3.5 by adding formic

135 acid. The resulting mixture was ultrasonically mixed for 5 min, vortexed and then centrifuged at 3000
136 g for 5 min to remove any precipitate.

137 2.3.3. Instrumentation, elution conditions and molecular weight calculation

138 The instrumental set-up and AF4 methods used for this work are the same as described earlier
139 (Pascotto et al., 2020). In brief, a Thermo Scientific Ultimate 3000 HPLC System, including degasser,
140 isocratic pump and autosampler, was used to inject samples and transport the mobile phase through the
141 system. The pump was coupled with the Eclipse AF4 (Wyatt Technology) to regulates flows in the
142 AF4 separation channel (long channel, Wyatt Technology Europe, Germany). The height of inserted
143 spacer of the AF4 channel was 350 μm and the membrane (Consensus, Germany) was in cellulose
144 material with a cut-off at 5 kDa. A multi-detection system including a UV-visible (set at $\lambda = 280$ and
145 230 nm), MALS, and a dRI, detectors (Wyatt Technology) was coupled with the AF4 system.
146 Chromeleon 6.8 software was used to control autosampler, pump and Eclipse flows. Acquisition of
147 UV, MALS and dRI data was performed using the Astra 6.1 software. Mobile phase used was
148 composed of 88% water (v/v) and 12% ethanol (v/v). Formic acid was added to adjust pH at 3.5. A
149 potassium salt was incorporated at 1 $\text{g}\cdot\text{L}^{-1}$ (K^+ equivalent) and 0.02% of sodium azide (s/v) was also
150 added to inhibit bacterial development. Wine samples were loaded to 400 μL in the AF4 channel. The
151 programs used to the wine sample and blank started with two minutes with the inlet flow at 1 $\text{mL}\cdot\text{min}^{-1}$
152 to obtain the baseline. Then, the relaxation step was applied for 8 min, against 6 min in the previous
153 paper (Pascotto et al., 2020). During this step, both the inlet and outlet channel flows were maintained
154 constant, at 1 $\text{mL}\cdot\text{min}^{-1}$ and 3 $\text{mL}\cdot\text{min}^{-1}$, respectively. Then, the elution step was started with a
155 crossflow (Q_c) = 3 $\text{mL}\cdot\text{min}^{-1}$, which was decreased exponentially (following equation 1) over time to
156 0.04 $\text{mL}\cdot\text{min}^{-1}$ and then maintained constant for 25 min.

$$157 \quad Q_c(\text{time}) = Q_c^{\text{end}} + (Q_c^{\text{start}} - Q_c^{\text{end}})e^{\frac{-\text{time}}{5}} \quad (1)$$

158 where, Q_c^{start} is the crossflow rate at the beginning of the elution step (3 $\text{mL}\cdot\text{min}^{-1}$), and Q_c^{end} is the
159 final crossflow rate targeted (0.04 $\text{mL}\cdot\text{min}^{-1}$). Each wine sample was preceded by a blank injection
160 and was followed by a cleaning program, injecting 100 μL of a solution of water/methanol (50:50)
161 before the next injection.

162 The weight average molecular weight (M_w) was calculated as described earlier (Pascotto et al., 2020).
163 Briefly, the M_w of compounds eluted in the F1 fractions was calculated using the dn/dc value reported
164 for tannins: 0.247 (Vernhet et al., 2011). Those of compounds eluted in fractions F2 and F3 were
165 calculated using the dn/dc value reported for polysaccharides, PRAGs and MPs: 0.146 (Redgwell,
166 Schmitt, Beaulieu, & Curti, 2005).

167 **2.4. Calculation of the polyphenol recovery rate by spectrophotometry**

168 The permeate fraction was recovered at the outlet of the crossflow during the relaxation step, using a
169 fraction collector AFC – 3000 (Thermo Scientific). Additionally, the retentate fraction was also
170 recovered during the elution step at the outlet-flow using a fraction collector Frac920, GE-Healthcare,
171 Sweden), positioned after the AF4 detectors. The permeate and retentate fractions were taken to
172 dryness with a Genevac EZ-2plus evaporator under reduced pressure at 8 mbars at 40 °C and freeze
173 dried. Then, both permeate and retentate dry powders were solubilized in 50 mL and 1 mL
174 respectively while the whole wine was diluted 200-fold in HCl (2%). Obtained sample solutions were
175 distributed in 96 wells (UV plate, Corning Life Sciences) and wells were filled with 170 μ L of the
176 sample. UV-visible absorbance was measured using a Nanoquant Infinite® 200 Pro spectrophotometer
177 (Tecan, Switzerland). Then, UV-visible spectra were acquired with 1 nm step, over the range 230 –
178 600 nm for each fraction and for the whole wine. Absorbance values at $\lambda = 280$ nm (A_{280}) and at $\lambda =$
179 230 nm (A_{230}) were extracted from the retentate and permeate fractions and the whole wine spectra.
180 The percentage of both A_{280} and A_{230} of the retentate and permeate fractions were calculated from
181 the absorbance values of the whole wine, representing 100% of the sample. Thus, the percentage of
182 recovery of the UV absorbing material was estimated for each analysis at 280 and 230 nm.

183 **2.5. Data processing**

184 *2.5.1. Sensory data*

185 The performances of the panel and of each judge were first evaluated. A three-way ANOVA with
186 interactions ($Y = \text{Wine} + \text{Judge} + \text{Repetition} + \text{Wine} \times \text{Judge} + \text{Wine} \times \text{Repetition} + \text{Judge} \times \text{Repetition}$
187 $+ \epsilon$ with $\alpha=5\%$) and a Generalized Products Analysis (GPA) were performed to assess the repeatability

188 of the judgements and to check the three main performances of a trained panel: discrimination,
189 consensus, and repeatability (Depledt, 2009). Both statistical treatments confirmed that the panel
190 fulfilled these requirements. Then, the data were treated to create groups of wines according to their
191 astringency intensity. First, a two-way ANOVA ($Y = \text{Wine} + \text{Judge} + \varepsilon$ with $\alpha=5\%$) and a difference
192 test (Fisher, LSD with $\alpha=5\%$) were performed to discriminate wines. Wines were separated into three
193 groups according to their mean score of astringency and the significant differences shown by the
194 Fisher-LSD test. First, thanks to the Fisher-LSD test, extreme samples, showing the lowest and the
195 highest astringency intensity were identified. Then, groups were created from this first observation, the
196 high intensity group was composed of wines non significantly different from the highest intensity
197 sample but significantly different from the lowest intensity one, and vice versa for the low intensity
198 group. Samples belonging to none of these groups were gathered in an intermediate intensity group.

199 2.5.2. *Cross-tabulation of the sensory and analytical data*

200 The analytical data obtained from the above-described methods were gathered in eight X tables, while
201 astringency scores were collected in the Y matrix (Table 1). The first eight minutes corresponding to
202 the elution step of the AF4 profiles were truncated to remove the unnecessary variables. Then, each
203 table was smoothed using a second-degree polynomial, 0-order. Due to the large number of variables
204 contained in the eight tables forming the X matrix, three variables were selected step by step from each
205 X table on the basis of their covariance with the astringency score (Y tables), using the *CovSel*
206 procedure (Roger, Palagos, Bertrand, & Fernandez-ahumada, 2011), under Chemflow web application
207 (<https://vm-chemflow-francegrille.eu/>) and were concatenated under X_{sel} table (Table 2). In addition,
208 both values of the percentage of retentate and permeate at 280 and 230 nm ($\%R280$, $\%R230$ and
209 $\%P280$, $\%P230$, respectively), were added to this table, independently to the *CovSel* procedure (Table
210 2). Then, principal component analysis (PCA) was performed under R, version 4.0.2, using factoextra
211 package, from X_{sel} table.

212 **3. *Results and discussion***

213 3.1. Sensory analysis

214 Quantitative Descriptive Analysis allowed discrimination of three groups of wines according to their
215 astringency. The ANOVA highlighted significant differences for the descriptor astringency (p-
216 value<0.001). Moreover, the fisher-LSD test also allowed to discriminate three groups (Fig.1): one
217 constituted by wines having a mean astringency score below 6.00 (“Low astringency samples” or
218 LAS); a second group having a score between 6.00 and 7.50 (“Medium astringency samples” or MAS)
219 and a third group of wines having a score over 7.50 (“High astringency samples” or HAS).

220 3.2. Chemical data analysis

221 3.2.1. Polyphenol recovery rate by spectrophotometry

222 Fig. 2 shows the distribution of recovery calculated over the 50 wine samples, for the permeate (%P),
223 the retentate (%R) and the sum of these two fractions, at 230 and 280 nm. Most of UV-absorbing
224 material of samples was removed through the channel membrane and recovered in the permeate (Fig.
225 2a, d) and the amount recovered in the retentate (%R) corresponded to ~2% for both wavelengths (Fig.
226 2b, e). Moreover, %P appeared lower at 230 nm (mean ~ 80%) than at 280 nm (~ 88%) whereas the
227 retained fraction (%R) seems to be slightly higher when measured at 230 nm than at 280 nm. These
228 two results suggest that the higher molecular mass UV-absorbing material can be distinguished from
229 the fraction eliminated in the permeate, by a shift of the maximum of absorbance. Furthermore, the
230 total recovery percentage was higher at 280 nm than at 230 nm, suggesting that the losses after
231 separation (through absorption on the membrane and/or during sample preparation and injection),
232 concern more the higher molecular weight compounds.

233 3.2.2. Description of UV-vis spectra and AF4 fractograms (X tables)

234 The UV-visible spectra of the whole wines, the permeate and retentate fractions are presented in Fig.
235 3a to 3c. The LAS, MAS and HAS astringency groups can be distinguished according to their
236 absorbance spectra showing low, intermediate, and high intensities, respectively, along the entire
237 spectrum for the retentate fractions and at lower wavelengths only for the entire wines. This suggests
238 that the retentate contains higher molecular weight phenolics that are astringent. The higher

239 absorbance values observed in the range 254-600 nm for the wine and permeate spectra reflect the
240 presence of phenolic compounds such as anthocyanins, flavonols, and phenolic acids which contribute
241 little to astringency and are recovered mostly in the permeate. Wine absorbance values at 230 nm also
242 appeared related to the astringency group, confirming earlier findings (Boulet, Ducasse, & Cheynier,
243 2017; Boulet et al., 2016).

244 The AF4 profiles of the 50 wines obtained with the three detectors and the molar mass distribution
245 (Figs. 3d to 3h) show the presence of several fractions as described earlier (Pascotto et al., 2020). The
246 first one (F1), eluted between two and five minutes, is clearly visible on the UV and dRI fractograms
247 and to a lesser degree on the MALS fractogram. It corresponds to higher molecular weight tannins
248 coeluted with RGII. Overall, the abundance of this fraction, especially in the UV profiles recorded at
249 280 nm (Fig. 3d) and 230 nm (Fig. 3e) increases in relation with the astringency level of wine,
250 consistent with the known contribution of higher molecular weight tannins to wine astringency.
251 Furthermore, RG-II has been shown to reduce perception of tannin astringency both in model solution
252 (Vidal et al, 2004) and in wine (Boulet et al, 2017), However, astringency seems mostly related to the
253 intensity of the UV signal and thus to the tannin concentration in F1, so that the effect of RGII cannot
254 be determined. Fractions (F2 and F3) are mostly visible on the MALS and dRI fractograms (Figs. 3f,
255 3g). These fractions, eluted between five and eight minutes and between eight and fifteen minutes,
256 respectively, have been attributed to intermediate (F2) and higher (F3) M_w polysaccharides (Pascotto
257 et al., 2020).

258 Moreover, the presence of UV absorbing material in these fractions could reflect the presence of
259 proteins or of polyphenols interacting with the polysaccharidic material. However, no relationship was
260 observed between the astringency level and their peak intensity or retention time. The fourth fraction
261 (F4) clearly visible on the MALS fractogram was eluted between fifteen and thirty minutes (Fig. 3f).
262 A great variability was observed from one sample to another for F4. It can be assumed that this
263 fraction was present in very small amount because the corresponding dRI or UV signal were close to
264 the baseline. Therefore, M_w could not be calculated for this fraction. However, the radius of gyration
265 (R_g) was determined from the MALS data and ranged from ~ 60 to 100 nm (data not shown). In

266 addition, for some samples, the MALS fractograms exhibited a fifth fraction (F5), eluting between 30
267 and 50 minutes, with a R_g = ranging from ~ 80 to 120 nm. Finally, the mean M_w calculated for F1, F2
268 and F3 varied between 7.5 and 23 kDa (F1), between 62 and 135 kDa (F2) and between 160 and 600
269 kDa (F3), respectively (Fig. 3g). The M_w of F1 increased with the astringency level while no clear
270 relationship was found for F2 and F3.

271 **3.3. Correlation between sensory and chemical data using multivariate analysis**

272 *3.3.1. Variable selection*

273 To avoid biases due to the huge number of variables in each spectrum or profile and high correlations
274 between them when performing PCA, three variables were independently selected from each X table,
275 on the basis of their correlation with the wine astringency scores, using the *CovSel* procedure (Roger
276 et al., 2011), as summarised in Table 2 and Fig. S1. The 230 nm wavelength was selected in all UV
277 spectra (retentate, permeate and whole wine), confirming the good potential of this wavelength to
278 predict the astringency scores (Boulet et al., 2016). However, the other wavelengths selected differed
279 according to the fraction. Indeed, a wavelength around 280 nm (277 nm) was only selected from the
280 retentate fraction spectra. It can be attributed to higher molecular weight tannins retained over the A4F
281 membrane which are known to be major contributors of wine astringency (Boulet et al., 2016;
282 Hufnagel & Hofmann, 2008a).

283 Other polyphenols such as anthocyanins, flavonols, and phenolic acids, contribute highly to the wine
284 absorbance around 280 nm (Boulet et al., 2017) but they were recovered mostly in the permeate.
285 Absorbances at 317 and 523 nm, reflecting the presence of phenolic acids and of anthocyanins,
286 respectively, were selected as the most relevant variables for astringency prediction in the permeate
287 spectra. Anthocyanins have been reported to increase wine astringency (Brossaud, Cheynier, & Noble,
288 2001) and interact with salivary proteins (Ferrer-Gallego et al., 2015). Phenolic acids have been
289 reported to contribute to astringency (Ferrer-Gallego et al., 2014; Hufnagel & Hofmann, 2008a; Peleg
290 et al., 1999; Vidal et al., 2018) and prediction of wine astringency was improved when taking their
291 concentration into account (Boulet et al., 2016). Absorbance at 313 nm selected in the wine spectra
292 also corresponds to phenolic acids or to coumaroylated anthocyanins.

293 These anthocyanins show higher affinity toward PVPP than non-acylated ones (Gil et al., 2017),
294 suggesting that they may be more astringent. Moreover, the 245 nm wavelength was selected in the
295 spectra of both whole wines and retentates among the variables most correlated with astringency. In
296 contrast, it was not selected in the permeate fraction (Table 2). This suggests that compounds
297 associated with absorbance at 245 nm, whose nature remains to be determined, do not have a major
298 impact on astringency when present as monomers or oligomeric molecules but contribute more
299 strongly when they are involved in larger polymers. Two variables selected from the 280 nm-UV
300 fractogram were localised in F1 and one in F2 (Table 2, Fig. S1), indicating that this data provided
301 information related to both the presence of tannins and of tannins interacting (or coeluted) with the
302 medium molecular mass polysaccharides such as PRAGs. However, all three variables selected from
303 the 230 nm-UV fractogram were in F1 (Table 2, Fig. S1). In contrast, the variables selected from the
304 MALS fractogram, were rather located in fractions F2/F3 and F4 (Table. 2, Fig. S1). This indicates
305 that this table brought variables related both to polysaccharidic compounds (F2/F3), and to unknow
306 compounds contained in F4, to explain the astringency scores.

307 Further, the variables selected from both dRI and M_w tables concern both fractions of tannins/RGII
308 and fractions containing polysaccharidic compounds (Table. 2, Fig. S1). Two variables relating to F1
309 and one to F3 were selected from the dRI table and one variable relating to the mass of F1 and two
310 relating to the masses of polysaccharides from the M_w table.

311 3.3.2. *Principal component analysis (PCA)*

312 Fig. 4 shows the distribution of individuals, coloured according to the astringency groups (a), and of
313 the quantitative variable groups (correlation circle, b) on the first plane of the PCA performed using
314 the variables selected from all tables. HAS wines were well separated from LAS wines along PC1
315 which was the component most influenced by the astringency groups (Fig 4a), Moreover, LAS
316 appeared better grouped compared to HAS or MAS, suggesting that these samples had more similarity
317 regarding analytical characteristics compared to other groups. Projection of variables on the
318 correlation circle (Fig 4b), shows that HAS were characterized with higher values of UV absorbance
319 of the retentate, variables associated to F1 in the AF4 fractograms (M_w at 3.7 min, dRI at 2.8 and 3.4

320 min, UV-280 and 230 nm at 3.2, 3.5, 3.8 min and 3.3, 3.8 respectively) and by the higher values of
321 recovery (%R at 280 and 230 nm).

322 These observations suggest that the abundance of F1 and the M_w of this fraction (compounds > 5 kDa)
323 increased substantially the perceived astringency in wine, as proposed earlier (Boulet et al., 2016).
324 Furthermore, the UV-280 nm variable selected at 7 min of retention time (corresponding to F2), was
325 also positively correlated to PC1, indicating that F2 from HAS absorbs highly in UV. F2 was already
326 identified to correspond to polysaccharidic fractions (Pascotto et al., 2020). This suggests that F2 in
327 HAS also contains very high molecular weight tannins. In contrast, LAS showed higher values of
328 variables related to F2/F3 (LS-9.2 min, M_w -9.6, and M_w - 13.0 min, dRI-8.2 min) and F4 (LS-21.7
329 and LS 26.9). This indicates that perceived astringency is counteracted by the polysaccharidic
330 material, as shown earlier (Boulet et al., 2016; Quijada-Morín et al., 2014), but also by the
331 compounds eluted in F4 which are not yet identified. In addition, it is interesting to note that the
332 impact of polysaccharides seems to increase with their M_w (Fig. 4b). Moreover, LAS were also the
333 samples having the highest absorbance values of permeate at 230 and 280 nm (%P230 and %P280).
334 This observation is consistent with the above discussed results showing that the most astringent wines
335 had the highest percentage of recovery (R%). MAS were highly dispersed and overlapped with both
336 HAS and LAS categories.

337 Two ways were envisaged. (i): This variability can be explained as the mean astringency scores,
338 determined by ANOVA were not significantly different from the other two groups. (ii): the presence
339 of proteins in the earlier retention time fractions, corresponding to F1 in this work, has been recently
340 shown (Marassi et al., 2020) and may contribute to the high intensity of F1 in UV absorbance. On the
341 other hand, PC2, was positively associated with absorbance values of the permeate fraction at 317 and
342 523 nm and of the wine, especially at 313 nm, but also to variables associated to the F4 fraction (LS-
343 21.7 and LS 26.9). Absorbance values at 313, 317, and 523 nm do not contribute to PC1 although they
344 have been selected on the basis of their correlation with the astringency scores, indicating that their
345 contribution to wine astringency is actually negligible compared to that of larger molecular weight
346 phenolic compounds eluted in F1. Furthermore, the whole wine wavelength group is relatively well

347 represented both on PC1 and PC2, meaning that this group of variables contributed to the separation of
348 individuals according to their astringency group (relative to PC1) and the dispersion of individuals on
349 PC2. It confirms that the information contained in the retentate and permeate spectra, which explained
350 the variability of the individuals with respect to PC1 and PC2 respectively, was averaged in whole
351 wines spectra.

352 **Conclusion**

353 Our results show that the profiles obtained on 50 red wines from the French Languedoc- Roussillon
354 region using the AF4-multidetector method described in our previous paper are related to astringency
355 scores determined by a trained sensory panel. The UV absorbing material in the colloid fraction
356 retained by the A4F membrane represented only a few percent of the absorbance measured on the
357 wines. However, red wine astringency was mostly related to retained (> 5kDa) polyphenols and
358 increased with their molecular weight while polyphenols eluted in the permeate fraction, although
359 much more abundant, had a negligible contribution. Lower astringency wines showed higher values of
360 variables related to F2, F3 and F4 in the MALS and M_w profiles, indicating that perceived astringency
361 was counteracted by the polysaccharidic material, in agreement with literature results, but also by
362 unknown compounds eluted in F4. Astringency softening also increased with polysaccharide M_w . The
363 AF4-multidetector method provides the first analysis of the red wine colloids contributing
364 astringency (i.e. higher molecular weight tannins) or mitigating it (i.e. polysaccharides and other
365 unknown polymeric material) in a single run. This paves the way for further investigation of the
366 colloidal material and mechanisms involved in red wine astringency.

367

368 *Acknowledgments*

369 The authors gratefully acknowledge the funding received from Occitanie Region, France and Ecole
370 d'Ingénieurs Purpan, Toulouse, France for the PhD fellowship of K. Pascotto and from Occitanie
371 Region, France for that of C. Leriche. The union of the Languedoc AOP and the Interprofessional
372 Association of Languedoc Wines are also thanked for providing the wine samples. People involved in

373 the experiments are gratefully acknowledged, in particular the judges of the sensory panel for their
374 contribution to astringency assessment, the winemakers who supplied the wines used for this work,
375 and D. Kleiber and G. Pasquier for helpful discussions.

376 *Literature cited*

377 Bate-Smith, E. C. (1973). Haemanalysis of tannins: The concept of relative astringency.
378 *Phytochemistry*, 12(4), 907–912. [https://doi.org/10.1016/0031-9422\(73\)80701-0](https://doi.org/10.1016/0031-9422(73)80701-0)

379 Baxter, N. J., Lilley, T. H., Haslam, E., & Williamson, M. P. (1997). Multiple interactions between
380 polyphenols and a salivary proline-rich protein repeat result in complexation and precipitation.
381 *Biochemistry*, 36(18), 5566–5577. <https://doi.org/10.1021/bi9700328>

382 Boulet, J.-C., Ducasse, M.-A., & Cheynier, V. (2017). Ultraviolet spectroscopy study of phenolic
383 substances and other major compounds in red wines: Relationship between astringency and the
384 concentration of phenolic substances. *Australian Journal of Grape and Wine Research*, 23(2),
385 193–199.

386 Boulet, J. C., Trarieux, C., Souquet, J. M., Ducasse, M. A., Caillé, S., Samson, A., Cheynier, V.
387 (2016). Models based on ultraviolet spectroscopy, polyphenols, oligosaccharides and
388 polysaccharides for prediction of wine astringency. *Food Chemistry*.
389 <https://doi.org/10.1016/j.foodchem.2015.05.062>

390 Brossaud, F., Cheynier, V., & Noble, A. C. (2001). Bitterness and astringency of grape and wine
391 polyphenols. *Australian Journal of Grape and Wine Research*, 7(1), 33–39.
392 <https://doi.org/10.1111/j.1755-0238.2001.tb00191.x>

393 Colonna A.E, Adams D.O, Noble A.C. (2004). Comparison of procedures for reducing astringency
394 carry-over effects in evaluation of red wines. *Australian Journal of Grape and Wine Research*,
395 10(1), 26–31. <https://doi.org/10.1111/j.1755-0238.2004.tb00005.x>

396 Deplédt Félix, M. J.-L. (2009). *Évaluation sensorielle (3e éd.)*. (Lavoisier Ed. Paris, Ed.).

397 Ferrer-Gallego, R., Hernández-Hierro, J. M., Rivas-Gonzalo, J. C., & Escribano-Bailón, M. T. (2014).

398 Sensory evaluation of bitterness and astringency sub-qualities of wine phenolic compounds:
399 Synergistic effect and modulation by aromas. *Food Research International*, 62, 1100–1107.
400 <https://doi.org/10.1016/j.foodres.2014.05.049>

401 Ferrer-Gallego, R., Soares, S., Mateus, N., Rivas-Gonzalo, J., Escribano-Bailón, M. T., & Freitas, V.
402 de. (2015). New Anthocyanin–Human Salivary Protein Complexes. *Langmuir*, 31(30), 8392–
403 8401. <https://doi.org/10.1021/acs.langmuir.5b01122>

404 Findlay, C. J., Castura, J. C., Schlich, P., & Lesschaeve, I. (2006). Use of feedback calibration to
405 reduce the training time for wine panels. *Food Quality and Preference*, 17(3–4), 266–276.
406 <https://doi.org/10.1016/j.foodqual.2005.07.005>

407 Gawel, R. (1998). Red wine astringency : Rewiev. *Australian Journal of Grape and Wine Research*,
408 74–95. <https://doi.org/https://doi.org/10.1111/j.1755-0238.1998.tb00137.x>

409 Gil, M., Avila-Salas, F., Santos, L. S., Iturmendi, N., Moine, V., Cheynier, V., & Saucier, C. (2017).
410 Rosé Wine Fining Using Polyvinylpolypyrrolidone: Colorimetry, Targeted Polyphenomics, and
411 Molecular Dynamics Simulations. *Journal of Agricultural and Food Chemistry*, 65(48), 10591–
412 10597. <https://doi.org/10.1021/acs.jafc.7b04461>

413 Harbertson James F, Kennedy J.A., Adams D.O. (2002). Tannin in Skins and Seeds of Cabernet
414 Sauvignon , Syrah , and Pinot noir Berries during Ripening, *J*(September 2001), 54–59.

415 Hufnagel, J. C., & Hofmann, T. (2008a). Orosensory-directed identification of astringent mouthfeel
416 and bitter-tasting compounds in red wine. *Journal of Agricultural and Food Chemistry*, 56(4),
417 1376–1386. <https://doi.org/10.1021/jf073031n>

418 Hufnagel, J.C., & Hofmann, T. (2008b). Quantitative reconstruction of the nonvolatile
419 sensometabolome of a red wine. *Journal of Agricultural and Food Chemistry*, 56(19), 9190–
420 9199. <https://doi.org/10.1021/jf801742w>

421 Kallithraka, S., Kim, D., Tsakiris, A., Paraskevopoulos, I., & Soleas, G. (2011). Sensory assessment
422 and chemical measurement of astringency of Greek wines: Correlations with analytical

423 polyphenolic composition. *Food Chemistry*, 126(4), 1953–1958.
424 <https://doi.org/10.1016/j.foodchem.2010.12.045>

425 Leriche, C., Molinier, C., Caillé, S., Razungles, A., Symoneaux, R., & Coulon-Leroy, C. (2020).
426 Development of a methodology to study typicity of PDO wines with professionals of the wine
427 sector. *Journal of the Science of Food and Agriculture*, 100(10), 3866–3877.
428 <https://doi.org/10.1002/jsfa.10428>

429 Macfie, H. J., Bratchell, N., Greenhoff, K., & Vallis, L. V. (1989). Designs To Balance the Effect of
430 Order of Presentation and First-Order Carry-Over Effects in Hall Tests. *Journal of Sensory*
431 *Studies*, 4(2), 129–148. <https://doi.org/10.1111/j.1745-459X.1989.tb00463.x>

432 Marassi, V., Marangon, M., Zattoni, A., Vincenzi, S., Versari, A., Reschiglian, P., et al (2021).
433 Characterization of red wine native colloids by asymmetrical flow field-flow fractionation with
434 online multidetection. *Food Hydrocolloids*, 110, 106204.
435 <https://doi.org/10.1016/j.foodhyd.2020.106204>

436

437 Mcrae, J. M., & Kennedy, J. A. (2011). Wine and Grape Tannin Interactions with Salivary Proteins
438 and Their Impact on Astringency: A Review of Current Research. *Molecules*, 16, 2348–2364.
439 <https://doi.org/10.3390/molecules16042348>

440 Nicod, H. (1998). *L'organisation pratique de la mesure sensorielle, l'entraînement*. (Lavoisier, Ed.)
441 (2nd ed).

442 Pascotto, K., Cheynier, V., Williams, P., Geffroy, O., & Violleau, F. (2020). Fractionation and
443 characterization of polyphenolic compounds and macromolecules in red wine by asymmetrical
444 flow field-flow fractionation. *Journal of Chromatography A*, 1629.
445 <https://doi.org/10.1016/j.chroma.2020.461464>

446 Peleg, H., Gacon, K., Schlich, P., & Noble, A. C. (1999). Bitterness and astringency of flavan-3-ol
447 monomers, dimers and trimers. *Journal of the Science of Food and Agriculture*, 79(8), 1123–

448 1128. [https://doi.org/10.1002/\(SICI\)1097-0010\(199906\)79:8<1123::AID-JSFA336>3.0.CO;2-D](https://doi.org/10.1002/(SICI)1097-0010(199906)79:8<1123::AID-JSFA336>3.0.CO;2-D)

449 Pellerin, P., Vidal, S., Williams, P., & Brillouet, J. M. (1995). Characterization of five type II
450 arabinogalactan-protein fractions from red wine of increasing uronic acid content. *Carbohydrate*
451 *Research*, 277(1), 135–143. [https://doi.org/10.1016/0008-6215\(95\)00206-9](https://doi.org/10.1016/0008-6215(95)00206-9)

452 Preys, S., Mazerolles, G., Courcoux, P., Samson, A., Fischer, U., Hanafi, M., et al. (2006).
453 Relationship between polyphenolic composition and some sensory properties in red wines using
454 multiway analyses. *Analytica Chimica Acta*, 563(1-2 SPEC. ISS.), 126–136.
455 <https://doi.org/10.1016/j.aca.2005.10.082>

456 Quijada-Morín, N., Williams, P., Rivas-Gonzalo, J. C., Doco, T., & Escribano-Bailón, M. T. (2014).
457 Polyphenolic, polysaccharide and oligosaccharide composition of Tempranillo red wines and
458 their relationship with the perceived astringency. *Food Chemistry*, 154, 44–51.
459 <https://doi.org/10.1016/j.foodchem.2013.12.101>

460 Redgwell, R. J., Schmitt, C., Beaulieu, M., & Curti, D. (2005). Hydrocolloids from coffee:
461 Physicochemical and functional properties of an arabinogalactan-protein fraction from green
462 beans. *Food Hydrocolloids*, 19(6), 1005–1015. <https://doi.org/10.1016/j.foodhyd.2004.12.010>

463 Roger, J. M., Palagos, B., Bertrand, D., & Fernandez-ahumada, E. (2011). Chemometrics and
464 Intelligent Laboratory Systems CovSel: Variable selection for highly multivariate and multi-
465 response calibration Application to IR spectroscopy. *Chemometrics and Intelligent Laboratory*
466 *Systems*, 106(2), 216–223. <https://doi.org/10.1016/j.chemolab.2010.10.003>

467 Soares, S., Brandão, E., Guerreiro, C., Soares, S., Mateus, N., & De Freitas, V. (2020). Tannins in
468 food: Insights into the molecular perception of astringency and bitter taste. *Molecules*.
469 <https://doi.org/10.3390/molecules25112590>

470 Stone and Sidel. (2004). *Quantitative Descriptive Analysis (The QDA method). Sensory evaluation*
471 *practices*. (C. Elsevier Academic Press, San Diego, Ed.) ((3rd ed.)).

472 Vernhet, A., Dubascoux, S., Cabane, B., Fulcrand, H., Dubreucq, E., & Poncet-Legrand, C. (2011).

473 Characterization of oxidized tannins: Comparison of depolymerization methods, asymmetric
474 flow field-flow fractionation and small-angle X-ray scattering. *Analytical and Bioanalytical*
475 *Chemistry*, 401(5), 1563–1573. <https://doi.org/10.1007/s00216-011-5076-2>

476 Vidal, L., Antúnez, L., Rodríguez-Haralambides, A., Giménez, A., Medina, K., Boido, E., & Ares, G.
477 (2018). Relationship between astringency and phenolic composition of commercial Uruguayan
478 Tannat wines: Application of boosted regression trees. *Food Research International*, 112(June),
479 25–37. <https://doi.org/10.1016/j.foodres.2018.06.024>

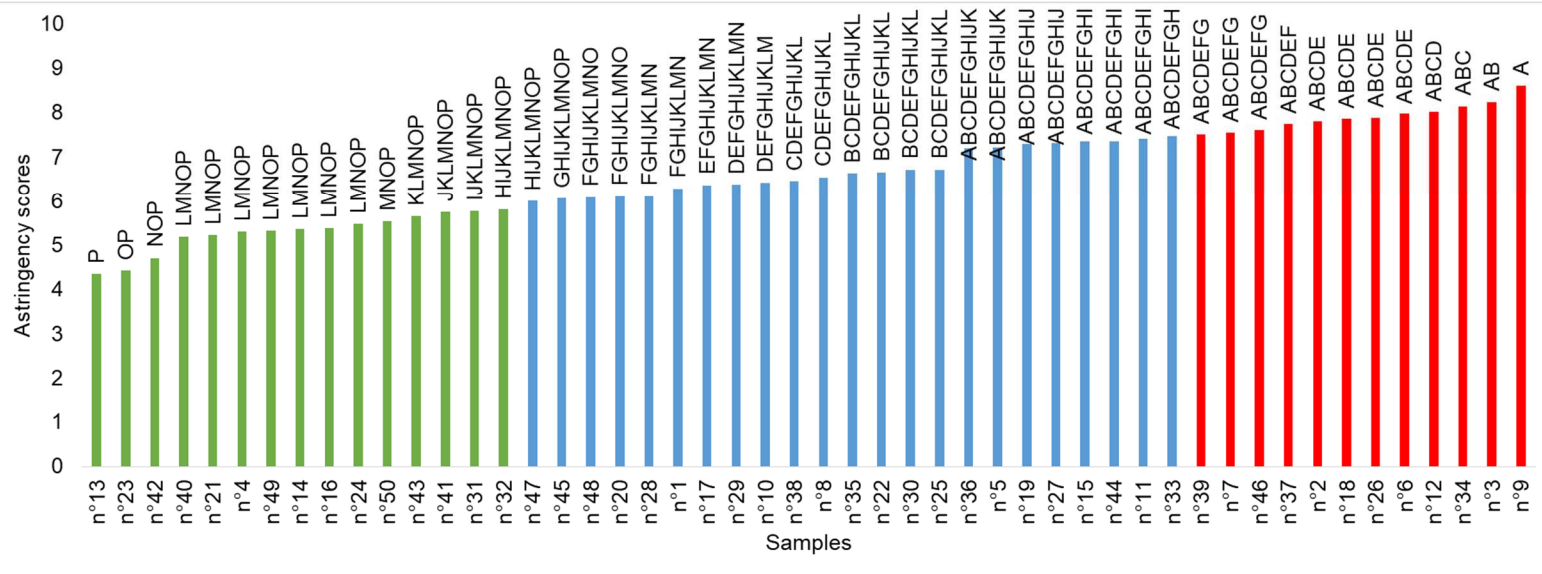
480 Vidal, S., Courcoux, P., Francis, L., Kwiatkowski, M., Gawel, R., Williams, P., et al. (2004). Use of
481 an experimental design approach for evaluation of key wine components on mouth-feel
482 perception. *Food Quality and Preference*, 15(3), 209–217. [https://doi.org/10.1016/S0950-](https://doi.org/10.1016/S0950-3293(03)00059-4)
483 [3293\(03\)00059-4](https://doi.org/10.1016/S0950-3293(03)00059-4)

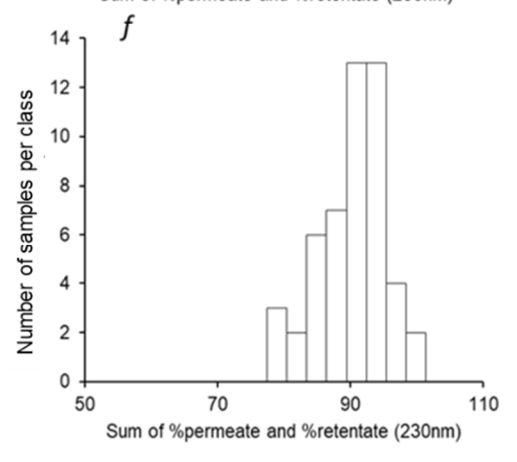
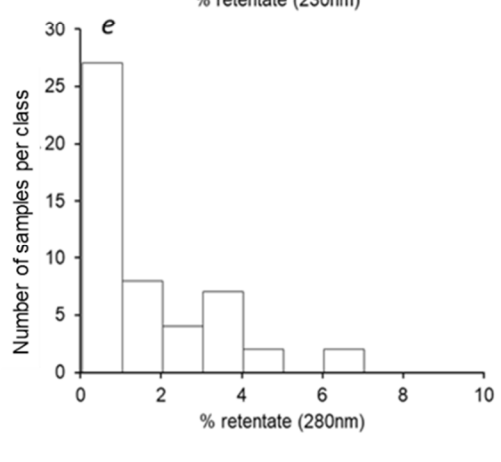
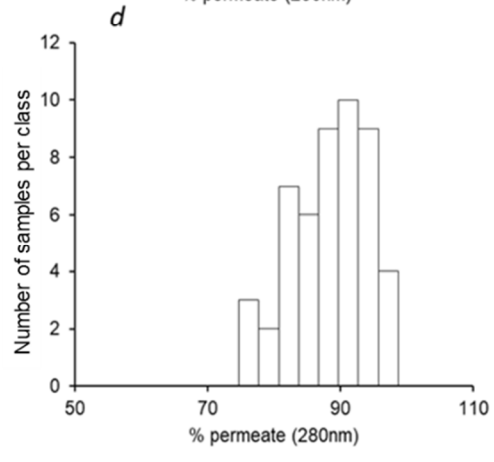
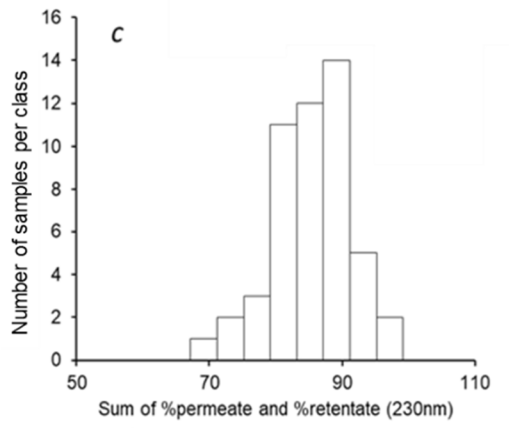
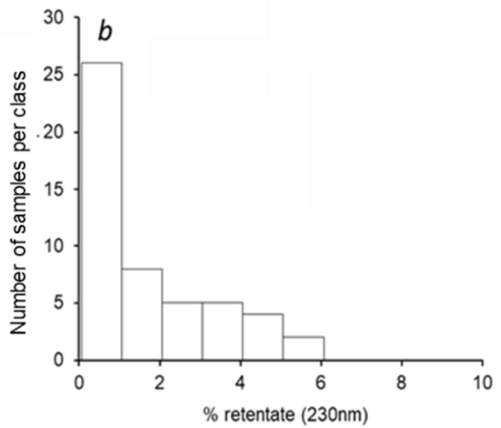
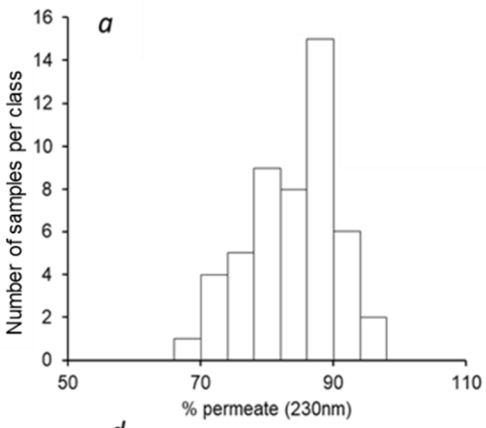
484 Vidal, S., Francis, L., Guyot, S., Marnet, N., Kwiatkowski, M., Gawel, R., et al. (2003). The mouth-
485 feel properties of grape and apple proanthocyanidins in a wine-like medium. *Journal of the*
486 *Science of Food and Agriculture*, 83(6), 564–573.
487 [https://doi.org/https://doi.org/10.1002/jsfa.1394](https://doi.org/10.1002/jsfa.1394)

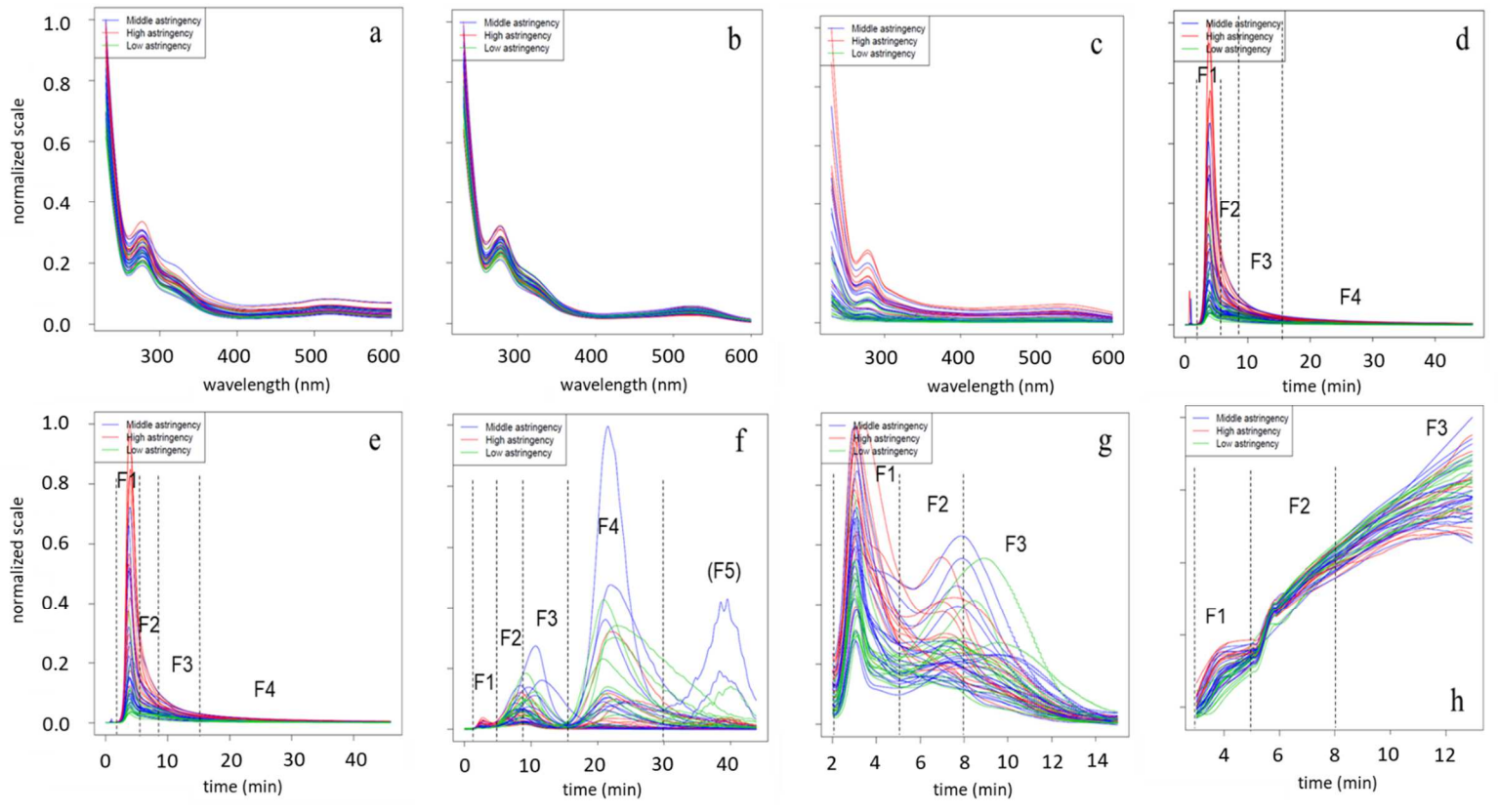
488 Vidal, S., Francis, L., Williams, P., Kwiatkowski, M., Gawel, R., Cheynier, V., & Waters, E. (2004).
489 The mouth-feel properties of polysaccharides and anthocyanins in a wine like medium. *Food*
490 *Chemistry*, 85(4), 519–525. [https://doi.org/10.1016/S0308-8146\(03\)00084-0](https://doi.org/10.1016/S0308-8146(03)00084-0)

491

492







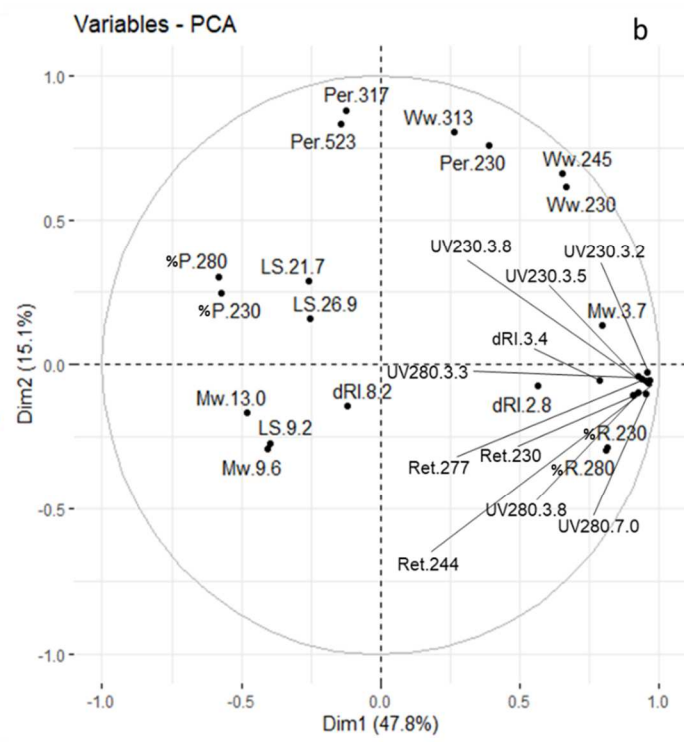
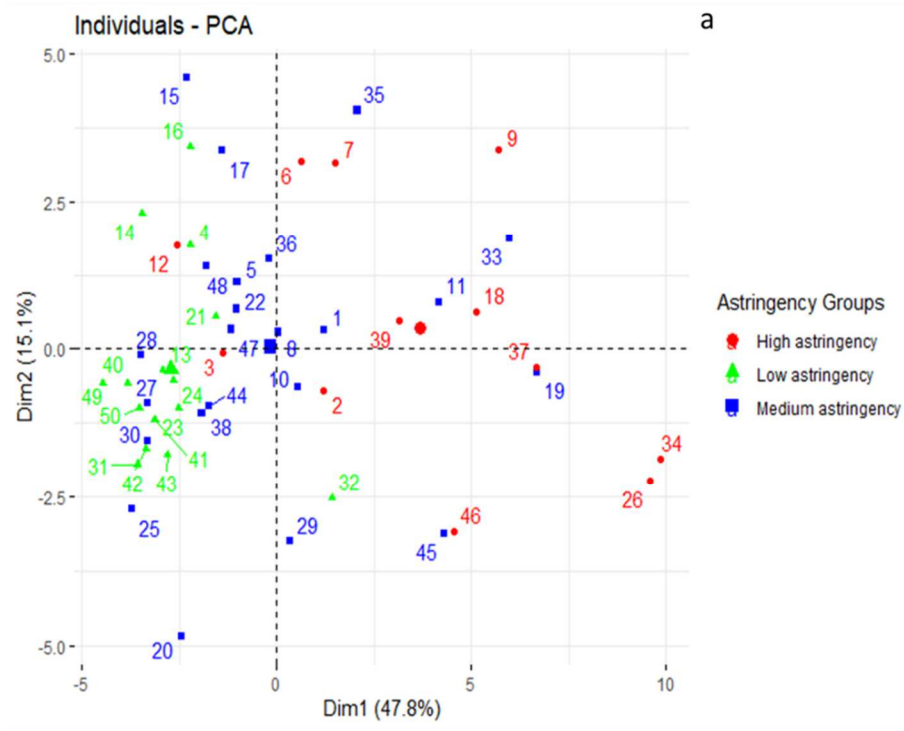


Table 1: Names, contents and dimensions of the *X* and *Y* tables included in data processing.

Name	Table	Dimensions (<i>n</i> x <i>p</i>) ^a	
<i>X1</i>	UV fractogram ($\lambda = 280\text{nm}$)	50 x 5521	
<i>X2</i>	UV fractogram ($\lambda = 230\text{nm}$)	50 x 5521	
<i>X3</i>	MALS fractogram (angle 90°)	50 x 2551	
<i>X</i>	<i>X4</i>	dRI fractogram	50 x 821
	<i>X5</i>	Log of weight average molecular weight distribution ($\text{Log}(M_w)$)	50 x 592
	<i>X6</i>	UV-vis spectra of retentate fraction	50 x 371
	<i>X7</i>	UV-vis spectra of permeate fraction	50 x 371
	<i>X8</i>	UV-vis spectra of whole wine	50 x 371
<i>Y</i>	astringency score	50 x 1	

^a n = number of samples, p = number of variables

Table 2: Identification of the three variables selected from each *X* table and their corresponding fractions.

Type	<i>X</i> table	Selected variable ^a	Variable name	Corresponding fraction	
AF4 fractogram	UV fractogram ($\lambda = 280\text{nm}$)	3.3	UV280-3.3	F1	
		3.8	UV280-3.8		
		7.0	UV280-7.0		
	UV fractogram ($\lambda = 230\text{nm}$)	3.2	UV230-3.2	F1	
		3.5	UV230-3.5		
		3.8	UV230-3.8		
	MALS fractogram (angle 90°)	MALS fractogram (angle 90°)	9.2	LS-9.2	F3
			21.7	LS-21.7	F4
			26.9	LS-26.9	
		dRI fractogram	2.8	dRI-2.8	F1
			3.4	dRI-3.4	
			8.2	dRI-8.2	
	Log of weight average molecular weight distribution ($\text{Log}(M_w)$)	3.7	Mw-3.7	F1	
9.6		Mw-9.6	F3		
13		Mw-13			
UV-vis spectra	UV-vis spectra of retentate fraction	230	Ret-230	-	
		244	Ret-244	-	
		277	Ret-277	-	
		230	%R 230	-	
		280	%R 280	-	
	UV-vis spectra of permeate fraction	230	Per-230	-	
		317	Per-317	-	
		523	Per-523	-	
		230	%P 230	-	
		280	%P 280	-	
	UV-vis spectra of whole wine	230	Ww-230	-	
		245	Ww-245	-	
		313	Ww-313	-	

^aThe dimension of variables is the time (min) and wavelength (nm) for the AF4 fractograms and UV-vis spectra, respectively.